SAND--96-1606C LA-UR- 96-1837
CONF-9607122--2

Momentum Transfer in Indirect Explosive Drive

J. E. Kennedy, Los Alamos National Laboratory,
C. R. Cherry, Sandia National Laboratories,
C. R. Cherry, Jr.
R. H. Warnes, Los Alamos National Laboratory,
S. H. Fischer, Sandia National Laboratories

Abstract

Material which is not in direct contact with detonating explosives may still be driven by the explosion through impact by driven material or by attachment to driven material. In such circumstances the assumption of inelastic collision permits estimation of the final velocity of an assemblage. Examples of the utility of this assumption are demonstrated through use of Gurney equations. The inelastic collision calculation may also be used for metal parts which are driven by explosives partially covering the metal. We offer a new discounting angle to account for side energy losses from laterally unconfined explosive charges in cases where the detonation wave travels parallel to the surface which is driven.

1. Introduction

The Gurney model and equations for predicting the velocity to which metal is driven by detonating explosives implicitly assume that the explosive is in contact with (all) the metal that is being driven. This paper addresses two geometries for which that assumption does not hold, and offers a method for predicting the behavior of these circumstances. The basic idea is that of inelastic collision; this amounts to momentum sharing between "primary" metal, which is directly driven by being in contact with the explosive, and "secondary" metal (not in contact with the explosive), which interacts with and travels with the primary metal.

We present experimental data which support this idea, and which also contain a surprise. The results of computational modeling and Gurney calculations provide insight into the surprising result.

2. Inelastic collision of free-flying plates and secondary objects

A range safety problem arose some years ago that was not described well by Gurney equations or by wave-code simulations because the system was rather complex. The problem was that of determining the maximum distance traveled by fragments from the detonation testing of a weapon assembly. In the weapon some relatively thin metal layers were driven through direct contact with the detonating explosive, and aerodynamic analysis indicated that fragments from these layers were not massive

enough to travel very far before being stopped by air drag. However, parts of these thin fragment layers impacted rather massive weapon components and drove those heavy components. The aerodynamic drag of the heavy components was proportionally so much less than that of the light ones that it became important to estimate the velocity to which the heavy components would be driven.

The idea which we applied for this analysis was that the light fragments would collide inelastically with the heavy component. It was postulated that the light and heavy pieces would then "stick together" and move off together with the momentum contributed by the initial velocity of the light fragments. Denoting mass and velocity respectively as M and v, the light fragment(s) as 1, the heavy component as 2, and the velocity of the combined mass as v_{1+2}, we then simply have

$$Momentum = M_1 v_1 = (M_1 + M_2) v_{1+2}. \qquad (1)$$

We argue for the conservation of momentum rather than energy because momentum can be conserved without having to create energy, but the converse is not true.

Light fragment velocities were calculated with Gurney equations and the air drag of the heavy components was estimated for tumbling flight (Ref. 1). Aerodynamic analysis predicted that the heavy components, driven by impact of light fragments, would travel farther than the faster free-flying light fragments, and this was indeed found to be true. The maximum distance predicted for a heavy component was 1786 ft. and the range measured for that component was 1746 ft. This exceeded the range of light fragments that were recovered. This good agreement suggests that this model for momentum transfer has merit.

3. Cherry Experiments

Another set of experimental data which involved indirect drive of some metal was generated by the Cherry family as part of a science fair project (Ref. 2). The efficiency of explosive slab charges of a fixed mass but different shapes was studied by Christopher Cherry, Jr. and his father, Christopher. The mass to be driven, a 4-in.-square , 3/4-in.-thick steel plate, was placed on top of a wooden post at a constant height of four feet, and leveled carefully. A charge of duPont Detasheet explosive weighing approximately 8.5 g and a rubber buffer sheet were attached to the rear face of the steel plate, as shown in Fig. 1. The charge was detonated by an electric blasting cap, and the distance which the plate flew before landing on a dirt road was measured. The rubber buffer was intended to prevent damage to the steel plate in the form of spallation or indenting of the plate;

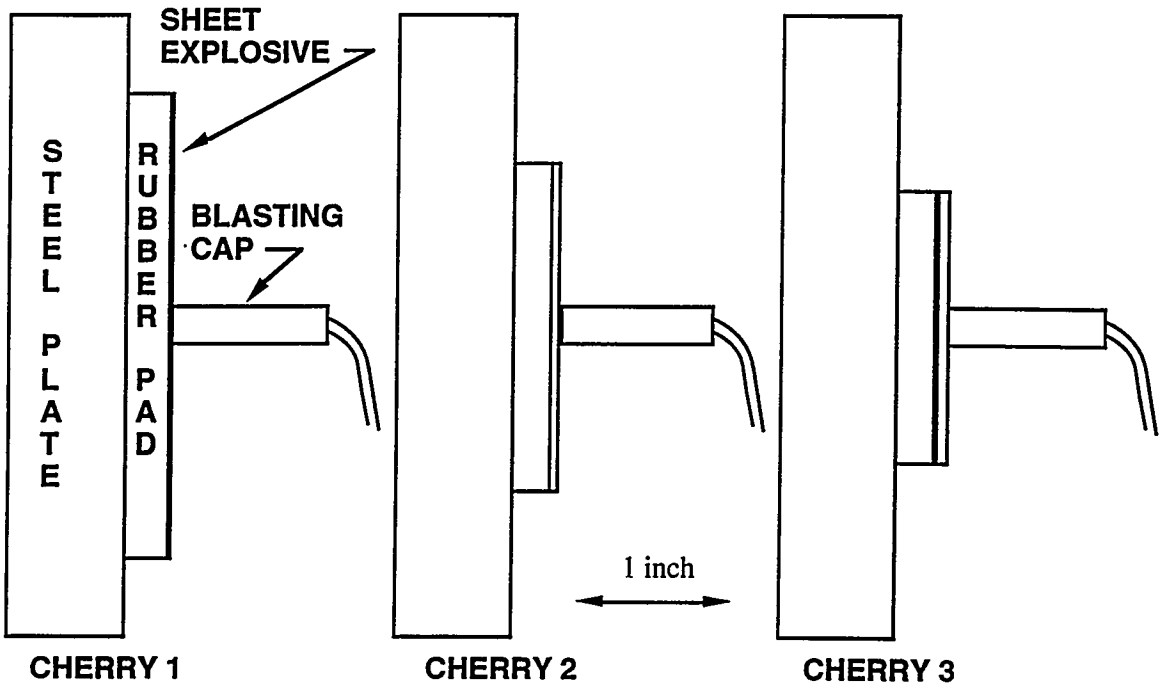

Fig. 1. Configuration of Explosive and Inert Parts of Cherry Experiments, to Scale

its use accomplished these objectives, and the Cherrys were able to use the same steel plate for the entire test series.

Experimental results were consistent for each charge shape, and are shown in Table I. The data show clearly that the thinnest charge, coveringthe greatest area on the plate surface, drove the plate to the highest velocity by a significant margin. This would not be expected on the basis of Gurney calculations of the plate velocity. If the entire plate mass and entire charge mass are used in an asymmetric-sandwich Gurney calculation (Ref. 3), the predicted velocity would be constant at 11.1 m/s for all three test configurations. The asymmetric-sandwich Gurney formula is

Table I

Results of Cherry Experiments Compared with Gurney Calculations

Experiment	Detasheet Explosive Size	Weight	Observed Velocity	Velocity by Gurney, Based on $\alpha^* = 30°$
Cherry 1	3 in. sq. x 0.042 in.	8.39 g	10.91 m/s	10.92 m/s
Cherry 2	2.125 in. sq. x 0.084 in.	8.65 g	9.66 m/s	10.93 m/s
Cherry 3	1.75 in. sq. x 0.126 in.	8.77 g	8.99 m/s	10.76 m/s

*Discounting angle, measured from a normal to the surface to be driven .

$$v = \sqrt{2E}\left[\frac{\left(1+2\frac{M}{C}\right)^3+1}{6\left(1+\frac{M}{C}\right)}+\frac{M}{C}\right]^{-\frac{1}{2}}, \qquad (2)$$

where M and C are the metal and explosive masses, respectively; $\sqrt{2E}$ is the Gurney velocity characteristic of Detasheet C, 2.50 km/s (Ref. 4); and v is the metal plate velocity. But the data show that the velocities varied with charge configuration, from 10.9 m/s to 9.0 m/s.

In regard to the velocity imparted to a driven plate, there are energy losses from the sides of an unconfined charge. One can account for these losses in a Gurney calculation by disregarding the explosive mass within a 30° angle from a normal to the plate around the perimeter of the explosive (Ref. 5). When such a correction is applied to the calculations for the Cherry experiments, the predicted velocity for all three configurations decreases, and the velocity for the thinnest charge decreases least of all. This trend is consistent with the experimental data, but the magnitude of the experimentally observed differences among configurations is much greater than the differences predicted by this correction. Velocities calculated with the 30°-angle correction are also shown in Table I.

3.1 Partial-area coverage with explosive

Our first attempt to model the variation in velocities among the Cherry experiments focused upon the variation in area of the explosive. It was assumed that the metal directly adjacent to the explosive charge was primary metal, driven directly by the explosive, and that the perimeter of the plate was secondary metal, carried along progressively through momentum sharing analogous to inelastic collision. Thus while the mass of explosive was constant in all three Cherry experiments, the mass of the primary metal was different for each experiment.

The asymmetric-sandwich formula (Eq. 2) was applied in this case. Note that the asymmetric sandwich formula collapses to a momentum form when $M/C >> 1$, and this applies to all of the Cherry experiments, even considering the reduced metal mass associated with the primary metal approach. This is shown from Eq. 2 as follows (Ref. 2):

$$\lim_{\frac{M}{C}\to\infty} v = \lim_{\frac{M}{C}\to\infty} \sqrt{2E}\left[\frac{\left(1+2\frac{M}{C}\right)^3+1}{6\left(1+\frac{M}{C}\right)}+\frac{M}{C}\right]^{-\frac{1}{2}} = \sqrt{2E}\cdot\sqrt{\frac{3}{4}}\cdot\frac{C}{M}. \qquad (3)$$

Specific impulse, I_{sp}, is defined as:

$$I_{sp} = \frac{Momentum}{C} = \frac{Mv}{C}, \tag{4}$$

so from Eqs. 3 and 4,

$$I_{sp} = \sqrt{1.5E}. \tag{5}$$

This indicates that for M/C >> 1 in an asymmetric sandwich configuration, the explosive delivers an impulse (momentum) that is linear with the explosive mass loading of the surface.

The momentum imparted to the primary metal in the Cherry experiments thus varies with the thickness of the explosive. But when the momentum of the primary metal is shared with the secondary metal, the final momentum of the plate is predicted to be the same in all three Cherry experiments. This result is not consistent with the observed velocities, so another approach is needed to explain the results.

3.2 Gasdynamics Behavior According to Wave-code Simulations

We performed wave-code computations to simulate the Cherry experiments for the purpose of understanding the gasdynamics which we postulated was causing the differences in performance. The question we addressed was whether the direction of detonation propagation was strongly affecting the effective side losses from the perimeter of the explosive charge. All three configurations of the Cherry experiments had configurations that were quite flat, so that the detonation resembled grazing detonation traveling nearly parallel to the surface of the plate and perpendicular to the sides of the charge. The detonation wave then projects gaseous detonation products parallel to the surface of the steel plate at a velocity approximately equal to detonation velocity. It was suspected that this velocity significantly exceeded the velocity of lateral expansion in the "normal" Gurney configuration, which we could represent as plane-wave initiation of the flat charges.

The CTH code, under development at Sandia (Ref.6), was used to perform two-dimensional axisymmetric representations of the experiments. For computational simplicity we converted the problem into a 2-D axisymmetric problem by modifying the shape of the steel plate, rubber buffer and explosive material to be right circular cylinders of the same respective masses. We used an equation of state for the detonation products of duPont Detasheet EL506C sheet explosive from Ref. 7.

When we included the rubber buffer layer in the problem, the code would essentially shut off before momentum transfer from the explosive to the steel plate was complete. This may have been due to rebound of the rubber from the steel, opening a gap into which the detonation product gases would flow. Such flow would cause tremendous distortion in the mesh for the product gases, and the distortion may have caused tangling of the computational mesh. It should be noted that the rubber buffer pad was found about 10-15 ft. behind the firing position in the experiments, indicating that the rubber did bounce backward off the steel.

Our next step was to eliminate the rubber from the problem description, so that the explosive rested directly on the steel. The steel description was modified to suppress spall behavior, so as to make the simulations consistent with the experimentally observed behavior in this regard.

Fig. 2 and Table II show the setup and results for computations done in this way. The computed velocity values shown in table II are low by about 25% in comparison with the experimental values. This is quite surprising, and we can only attribute it to probable error in the JWL parameters for Detasheet C. We shall use the computed velocity results only for comparison with other computed results, and not in any absolute sense.

Fig. 2 also compares the flow of product gases at the same time interval after completion of detonation of the charge for the cases of small area initiation (similar to the experiment) and planar initiation. The results show that lateral expansion of the gas is indeed faster with small area initiation, which produces grazing detonation, but only by a factor of about 1.2.

Table II shows the computed metal velocity differences that are caused by the differences in lateral expansion, which should be viewed as a

Table II

Results of CTH Wavecode Analysis of Cherry Experiments

Configuration	Initiation	Computed Velocity	Observed Velocity
Cherry 1	Small area	8.01 m/s	10.91 m/s
	Planar	7.99 m/s	
Cherry 2	Small area	7.68 m/s	9.66 m/s
	Planar	7.89 m/s	
Cherry 3	Small area	7.35 m/s	8.99 m/s
	Planar	7.72 m/s	

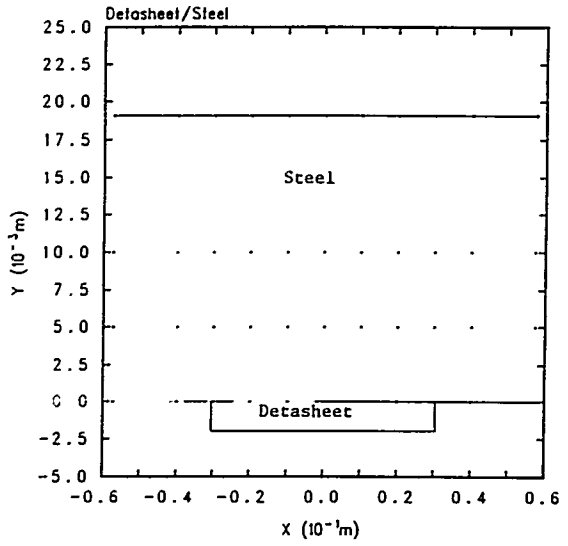

(a)

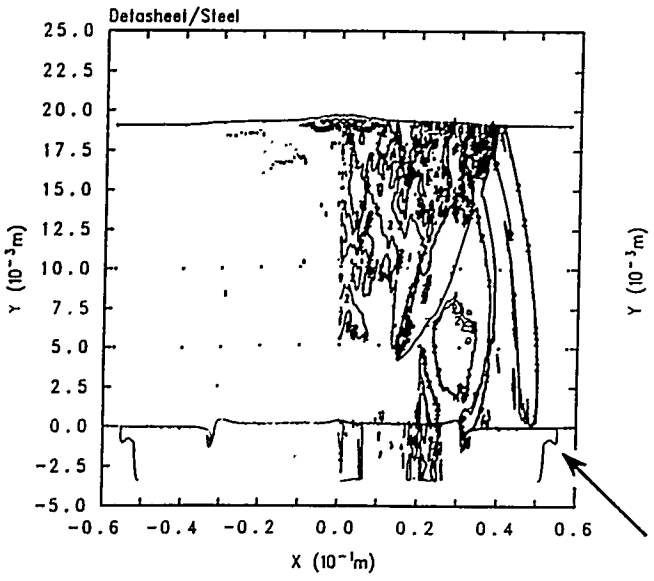

(b)

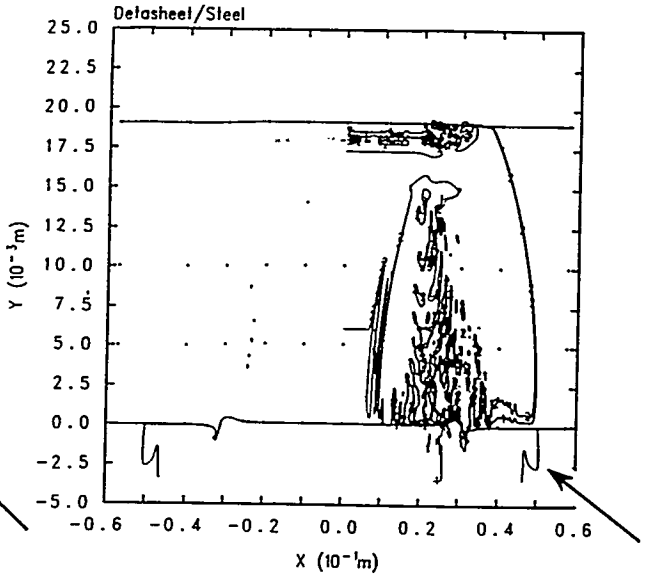

(c)

Fig. 2. (a)—The initial configuration of one of the CTH calculations. (b)—A two-dimensional plot of the small-area initiation of the Detasheet at a time when the gas expansion wave is approaching the outer edge of the steel (denoted by the arrow). (c)—A two-dimensional plot of the full-back-surface initiation of the Detasheet, showing the position of the gas expansion wave at an equivalent time from explosive breakout to that in (b), see arrow.

loss mechanism in regard to momentum transfer to the plate. The result is that planar initiation drives the plate to higher velocity, but only by 3-5% more than small area initiation (and grazing detonation). The difference in computed velocity between Cherry 1 and Cherry 3 configurations is 8%; this is substantially less than the differences in velocity observed among the experiments, which are shown again in Table II.

The difference in computed plate velocity in cases where detonation was parallel to the driven surface (grazing detonation) and where detonation was normal to the driven surface suggests that the loss factor be increased when the detonation is parallel to the driven surface. Based upon the results in Table II, we conclude that use of a discounting angle of 36° would improve the ability of the Gurney model to reproduce computed results when detonation of a laterally unconfined charge proceeds parallel to the surface which is being driven.

3.3 Inelastic Collision Modeling of Cherry Experiments

The rubber buffer pads caused some decoupling of the detonation wave from the steel because the rubber impedance was much lower than that of both the detonating explosive and the steel. The thickness of the rubber pad was constant at 1/4 in. in these experiments, and the rubber was the same area as the explosive, which varied from one Cherry experiment to another. Thus the mass of the rubber varied from one Cherry experiment to the next. This suggested the possibility that the variation in mass of the rubber played a role in the variation in coupling from the explosive to the steel plate in the Cherry experiments.

Although the rubber buffer pads were in contact with both the explosive and the steel plate, we carried out a bounding calculation using the asymmetric-sandwich Gurney formula (Eq. 2) in which the explosive was assumed to drive the rubber alone, and then the rubber was assumed to collide inelastically with the steel (Eq. 1). The results of this calculation, which uses a Gurney discounting angle of 36° (see Fig. 3), are shown in Table III.

Table III
Results of Inelastic Collision with Driven Rubber Buffer

Configuration	Rubber Buffer		Plate Velocity by	Observed
	Weight	Velocity*	Inelastic Collision	Velocity
Cherry 1	36.8 g	428 m/s	9.42 m/s	10.91 m/s
Cherry 2	18.5 g	762 m/s	8.53 m/s	9.66 m/s
Cherry 3	12.5 g	1012 m/s	7.68 m/s	8.99 m/s

*Calculated by asymmetric sandwich formula, Eq. 2, with M = rubber buffer mass.

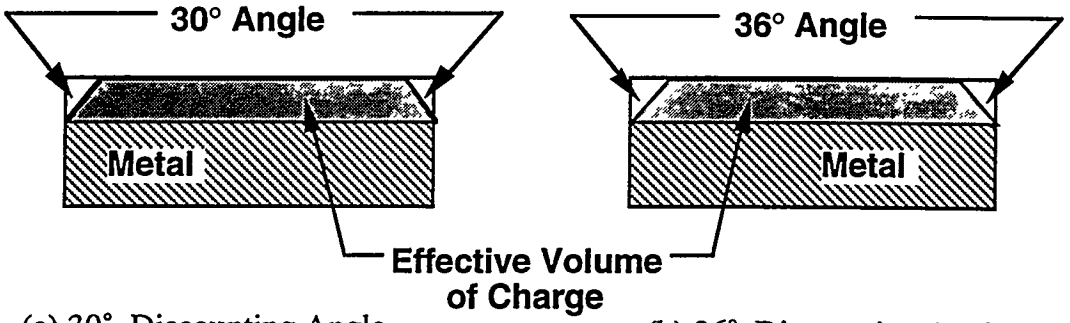

(a) 30° Discounting Angle (b) 36° Discounting Angle

Fig. 3. Discounting angle for laterally unconfined charge is increased from 30° to 36° when detonation wave travels parallel to the metal surface being driven.

The values of the steel plate velocity are lower than the observed values by 12-15%, but the calculated differences in velocities are quite similar to the observed differences. The inelastic collision assumption is the only analysis that reflects the differences in velocity among the three Cherry experiments. Therefore we conclude that the rubber decoupling is the dominant factor in the behavior of the Cherry experiments, and this analysis represents another example of the usefuness of the inelastic collision model. As an explanation for the fact that observed velocities are higher than those predicted by the inelastic collision model, we suggest that some additional impulse is imparted by the detonation product gas pressure acting over the entire area of the steel plate at relatively late times in the process.

(It should be noted that one of us (C.R.C.) offers another explanation for the differences among Cherry 1, 2, and 3. He suggests that the layers of explosive further from the surface of the steel plate are less effective than that which is in contact with the plate, resulting in the observation that the Cherry 3 configuration is less efficient than Cherry 1. This is consistent with the discounting angle effect, and would require a discounting angle of about 56° to correlate with the data. Such a large discounting angle is not consistent with the computed results shown in Table II.)

4. Summary

The findings of this research are as follows.

• To calculate the velocity of metal configurations that are driven indirectly by explosive detonation, the use of an **inelastic collision model** provides good results and insight into the interaction process. This model applies for metal that is directly driven by the explosive, and then impacts and travels along with other objects. We recommend that it be applied for plates or other shapes which are partially in contact with explosive, where the entire body remains intact (i.e., does not shear). It even worked better

than other models to explain decoupling of detonation drive from a heavy steel plate by the use of a rubber buffer plate inserted between the explosive and the steel plate.
• Based upon the results of computer simulation, we recommend the use of a 36° discounting angle (rather than the conventional 30° discounting angle) for laterally unconfined charges in which the detonation wave travels parallel to the surface to be driven.

References

1. H. Spahr, S. H. Fischer and J. E. Kennedy, Sandia National Laboratories unpublished results, 1984.
2. C. R. Cherry, Jr., "Determining the Propulsive Efficiency of a Geometrically Shaped High Explosive Charge," Report to Hope Christian School, Grade 8, Albuquerque, NM, 1995.
3. J. E. Kennedy, "Gurney Energy of Explosives: Estimation of the Velocity and Impulse Imparted to Driven Metal," Sandia National Laboratories Report SC-RR-70-790, Albuquerque, NM, Dec., 1970.
4. J. Roth, Portola Valley, CA, private communication, 1971.
5. F. A. Baum, K. Stanyukovich and B. I. Shekhter, Physics of an Explosion, p. 505-507, Moscow, 1959 (English translation from Federal Clearinghouse AD 400151).
6. R. L. Bell, M. G. Elrick, E. S. Hertel, G. I. Kerley, J. M. McGlaun, S. A. Silling, P. A. Taylor, and S. L. Thompson, "CTH User's Manual and Input Instructions, Version 2.00," Albuquerque, NM, Aug. 19, 1994.
7. B. M. Dobratz and P. C.. Crawford, LLNL Explosives Handbook: Properties of Chemical Explosives and Explosive Simulants, Lawrence Livermore National Laboratory Report UCRL-52997 Change 2, Jan. 31, 1985.

DISCLAIMER